Phase-modulation laser spectroscopy

Axel Schenzle,* Ralph G. DeVoe, and Richard G. Brewer
IBM Research Laboratory, San Jose, California 95193
(Received 16 November 1981)

A novel phase-modulation technique which permits subkilohertz-laser stability and new levels of precision in laser spectroscopy was reported recently. For spectroscopy, the basic arrangement consists of a combination of an optical pump and a probe field which is phase modulated. The pump prepares the atomic sample by burning a narrow hole within the atom's inhomogeneous line shape, and the probe beam samples the prepared hole when its modulation sidebands are swept into resonance. Off resonance, the probe is balanced as pairs of sidebands produce heterodyne beat signals of opposite phase which just cancel. On resonance, the balance is upset and yields a nonvanishing beat signal with a Lorentzian absorption or dispersion line shape and with residual noise approaching the shot noise limit. Here we investigate the theory of phase-modulation spectroscopy. We treat the nonlinear response of an atomic two-level quantum system subject to an intense pump and a weak copropagating or counterpropagating phase-modulated probe beam. The density-matrix equations of motion are solved by a Laplace-transform method and by the novel use of a translation operator which allows the infinite hierarchy of coupled equations to close. A solution equivalent to the rate-equation result is developed and coherence corrections are found which predict new resonances that have just been detected in this laboratory. The delayed pump-probe technique encountered in solid-state laser spectroscopy is analyzed in this context for two- and three-level quantum systems. The response of a Fabry-Perot cavity to a phase-modulated light wave is examined also and reveals an unexpected absorption feature.

I. INTRODUCTION

An elegant phase-modulation method for detecting optical atomic resonances, particularly in the nonlinear regime, has been devised recently[1–3] and applied to phase locking a laser to a reference cavity with unsurpassed precision.[2–4] Laser phase locking has produced a laser linewidth as narrow as ~ 100 hertz in the case of a dye laser[2] and is also being used in an attempt to detect gravity waves with optical interferometers.[5] While these detection ideas are new in the optical region, far earlier developments at longer wavelengths exist. Thus, Smaller[6] demonstrated some thirty years ago the advantages of phase modulation in (linear) magnetic resonance spectroscopy. Even earlier, Pound[7] proposed that microwave oscillators could best be stabilized by phase locking. Phase-modulation spectroscopy also resembles the heterodyne detection utilized in coherent optical transients where laser frequency switching is employed.[8]

The basic spectroscopic arrangement considered here consists of a combination of optical pump and probe fields which appear either simultaneously or in sequence. The pump is typically a single frequency cw laser field that prepares an atomic sample, for example, by burning a hole within its inhomogeneous line shape. The probe, which can be derived from the pump or another laser source, is phase modulated and therefore contains a Bessel function distribution of sidebands that appear symmetrically in pairs about the unmodulated laser frequency.

In the absence of attenuation, each pair of sidebands generates with the central frequency component at a photodetector a pair of heterodyne beat signals of opposite phase which just cancel. This balance is upset and a nonvanishing beat signal remains when the probe frequency is swept, bringing a sideband into resonance with the prepared hole. The background signal and its noise are therefore eliminated automatically. Moreover, since the beat frequency can be made arbitrarily high (radio or microwave), the desired beat signal can be detected in a spectral region where the residual noise spectrum is falling off. The resulting high sensitivity, which will ultimately be limited by shot noise, promises new levels of precision in laser spectroscopy.

 ©1982 The American Physical Society

In this article, we investigate the theory of phase-modulation laser spectroscopy, extending the work of Bjorklund[1(a)] and Hall *et al.*[3] Our analysis treats the nonlinear optical response of a two-level atomic quantum system subject to copropagating or counterpropagating laser beams where at least one of the fields is phase modulated. The counterpropagating beam case resembles the Lamb-dip effect but is more complex due to the multimode character of the phase-modulated probe. Solutions equivalent to a rate-equation result are developed and the effect of coherence corrections are examined, revealing in certain cases new resonances. The delayed pump-probe measurement frequently encountered in solid-state optical-hole-buring studies is analyzed where it is found that the two- and three-level quantum systems behave differently. Finally, the (linear) response of a Fabry-Perot cavity to a phase-modulated light wave is considered because of its relevance to phase locking a laser.

II. BASIC THEORY

A. Equations of motion: counterpropagating beams

We treat the nonlinear optical response of an atomic two-level quantum system subject to two collinear light fields that propagate in opposite directions along the laboratory z axis. The one field,

$$E_1(z,t)=\tilde{E}_1 e^{i(\omega_0 t+kz)}+\text{c.c.}\ , \tag{2.1}$$

we designate the pump field. The counterpropagating component, the probe field

$$E_0(z,t)=\tilde{E}_0 e^{i(\omega_0 t-kz)} e^{i\varphi(t)}+\text{c.c.}\ , \tag{2.2}$$

is phase modulated at frequency Ω where

$$\varphi=M\cos\Omega t\ ,$$

and therefore possesses sidebands according to the Fourier decomposition

$$e^{i\varphi(t)}=\sum_{n=-\infty}^{\infty} a_n e^{in\Omega t}\ . \tag{2.3a}$$

Here, $a_n=i^n J_n(M)$, J_n is the nth-order Bessel function,

$$a_n=a_{-n} \text{ and } a_n^*=(-1)^n a_n\ . \tag{2.3b}$$

Both fields are assumed polarized along the x axis. To account for the atom's motion with velocity v_z, and hence its time dependence, we transform from the laboratory (z) to the atom's moving coordinate (z') by

$$z=z'+v_z t\ .$$

The total field can then be written in the compact form

$$\begin{aligned}E(z',t)&=E_0(z',t)+E_1(z',t)\\ &=e^{i(\omega_0-kv_z)t}\sum_{n,m} A_n^m e^{i\Omega_n^m t}+\text{c.c.}\ ,\end{aligned} \tag{2.4}$$

where the pump field is specified by $m=1$,

$$A_0^1=\tilde{E}_1 e^{ikz'} \text{ and } \Omega_0^1=2kv_z,\quad n=0\ , \tag{2.5}$$

and the probe field by $m=0$,

$$A_n^0=\tilde{E}_0 e^{-ikz'} a_n$$

and

$$\Omega_n^0=n\Omega,\quad n=0,\ \pm 1,\ \pm 2,\ \ldots\ . \tag{2.6}$$

Thus, it is assumed that the two fields are present simultaneously, whereas in Sec. III the simpler problem of pump and probe occupying different time intervals is considered. We ignore the slight difference in pump and probe k vectors ($\Delta k=\Omega/c$) arising from phase modulation and assume in (2.5) and (2.6) that $k\equiv k_0^1=k_n^0$. Also, the slowly varying components of (2.4) are given by

$$\tilde{E}^+(t)=\sum_{n,m} A_n^m e^{i\Omega_n^m t} \text{ and } \tilde{E}^-=(\tilde{E}^+)^*\ . \tag{2.7}$$

In addition, (2.4) is sufficiently general to allow phase modulation in each of the counterpropagating beams, a case we treat later.

The density-matrix equations of motion

$$i\hbar\frac{\partial\rho}{\partial t}=[H,\rho]+\cdots\ ,$$

where the ellipsis represents damping terms for a two-level quantum system, with upper level 2 and lower level 1, can now be written[9] as

$$\begin{aligned}\frac{d}{dt}\tilde{\rho}_{12}(t)=&\,(i\Delta-1/T_2)\tilde{\rho}_{12}\\ &-2igw\sum_{n,m} A_n^m e^{i\Omega_n^m t}\ ,\end{aligned} \tag{2.8a}$$

$$\begin{aligned}\dot{w}(t)=&-ig\left[\tilde{\rho}_{12}\sum_{n,m} A_n^{m*} e^{-i\Omega_n^m t}-\tilde{\rho}_{21}\sum_{n,m} A_n^m e^{i\Omega_n^m t}\right]\\ &-(w-w^0)/T_1\ .\end{aligned} \tag{2.8b}$$

Here, the atomic unperturbed energy eigenvalues are

$$H_{11}=\hbar\omega_1,\ H_{22}=\hbar\omega_2\ ,$$

and

$$\omega_{21}\equiv\omega_2-\omega_1\ ,$$

while the off-diagonal optical-atom interaction is

$$H_{12}=g\hbar E(z,t)\ , \tag{2.9}$$

with

$$g=-\mu_{12}/\hbar\ , \tag{2.10}$$

μ_{12} being the dipole matrix element. In (2.8), we have applied the rotating wave approximation and retained the slowly varying off-diagonal component $\tilde{\rho}_{12}$ with the substitution

$$\rho_{12}=\tilde{\rho}_{12}e^{i(\omega_0-kv_z)t}\ . \tag{2.11}$$

The tuning parameter is defined as

$$\Delta=\omega_{21}-\omega_0+kv_z\ , \tag{2.12}$$

the population difference as

$$w=\tfrac{1}{2}(\rho_{22}-\rho_{11})\ , \tag{2.13}$$

and the phenomenological dipole (T_2) and population (T_1) decay times have been introduced.

The pump and probe fields generate a signal field

$$\tilde{E}_s^{+}\rightsquigarrow ig\langle\tilde{\rho}_{12}(z',t)\rangle\ , \tag{2.14}$$

where the directionality of the beam, as we shall see, appears in the solution $\tilde{\rho}_{12}(z',t)$ due to the $e^{\pm ikz'}$ phase factors of (2.5) and (2.6). Equation (2.14) is valid for an optically thin sample and follows from Maxwell's wave equation in the slowly-varying envelope approximation. The angle bracket of (2.14) indicates an average

$$\langle\tilde{\rho}_{12}\rangle=\int_{-\infty}^{\infty}G(v_z)\tilde{\rho}_{12}(v_z)d(kv_z) \tag{2.15}$$

over the inhomogeneous line shape where

$$G(v_z)=e^{-(v_z/u)^2}/(\sqrt{\pi}ku)$$

for an atomic system, u being the most probable velocity. Equation (2.15) is to be evaluated in the limit of infinite Doppler width, an assumption which is valid in optical-hole-burning experiments.

However, the observable is a heterodyne beat of the signal field (2.14) and the total field (2.4) where the cross terms of the intensity $|E(t)+E_s(t)|^2$ are

$$B(t)=\tilde{E}^{+}\tilde{E}_s^{-}+\tilde{E}^{-}\tilde{E}_s^{+}\ . \tag{2.16}$$

B. Laplace transform

The equations of motion (2.8) constitute a set of three linear differential equations with time-dependent coefficients. These can be solved by use of the Laplace transform[10]

$$\rho(Z)=\int_0^{\infty}e^{-Zt}\rho(t)dt\ , \tag{2.17}$$

where the inverse transform is given by

$$\rho(t)=\frac{1}{2\pi i}\int_{-i\infty+r}^{i\infty+r}e^{Zt}\rho(Z)dZ\ . \tag{2.18}$$

By application of (2.17), Eqs. (2.8) become

$$\tilde{\rho}_{12}(Z)=\frac{-2ig}{Z-i\Delta+1/T_2}\sum_{n,m}A_n^m w(Z-i\Omega_n^m)\ , \tag{2.19a}$$

$$w(Z)(Z+1/T_1)=\frac{w^0}{ZT_1}-ig\sum_{n,m}A_n^{m*}\tilde{\rho}_{12}(Z+i\Omega_n^m)+ig\sum_{n,m}A_n^m\tilde{\rho}_{21}(Z-i\Omega_n^m)\ . \tag{2.19b}$$

Here, the initial conditions are not retained as only the long-time behavior ($t>>T_2$) is of interest. Notice that Eqs. (2.19) do not close on one another but instead form an infinite hierarchy of coupled equations involving terms of the type

$$\tilde{\rho}_{12}(Z\pm i\Omega_n^m),\tilde{\rho}_{12}(Z\pm 2i\Omega_n^m),\tilde{\rho}_{12}(Z\pm 3i\Omega_n^m),\ldots\ .$$

This difficulty is formally avoided by introducing the translation operator[11]

$$T(X)f(Z)=f(Z+iX)\ , \tag{2.20}$$

where

$$T(X)=\sum_n\frac{(iX)^n}{n!}\frac{\partial^n}{\partial Z^n}\ ,$$

and it is evident that

$$T(X)T(Y)=T(X+Y)\ . \tag{2.21}$$

The hierarchy of Eqs. (2.19) can now be written in a compact form which closes, namely,

$$\tilde{\rho}_{12}(Z)=\frac{-2ig}{Z-i\Delta+1/T_2}\sum_{n,m}A_n^m T(-\Omega_n^m)w(Z)\ , \tag{2.22a}$$

$$w(Z)(Z+1/T_1)=\frac{w^0}{ZT_1}-ig\sum_{n,m}A_n^{m*}T(\Omega_n^m)\tilde{\rho}_{12}(Z)+ig\sum_{n,m}A_n^m T(-\Omega_n^m)\tilde{\rho}_{21}(Z)\ . \tag{2.22b}$$

However, the problem of dealing with noncommuting operators must be faced. We find from (2.22b), after inserting $\tilde{\rho}_{12}(Z)$ and $\tilde{\rho}_{21}(Z)$ from (2.22a) and then using (2.21), that

$$w^0/ZT_1=\left[Z+1/T_1+4g^2\sum_{\substack{n,n'\\m,m'}}\Lambda_{nn'}^{mm'}(Z)A_n^{m*}A_{n'}^{m'}\,T(\Omega_n^m-\Omega_{n'}^{m'})\right]w(Z)\ , \tag{2.23}$$

where

$$\Lambda_{n,n'}^{m,m'}(Z)=\tfrac{1}{2}[(Z-i\Delta+i\Omega_n^m+1/T_2)^{-1}+(Z+i\Delta-i\Omega_{n'}^{m'}+1/T_2)^{-1}]\ . \tag{2.24}$$

C. Rate equations

At this point, it becomes necessary to introduce approximations, as the general analytic treatment developed thus far cannot be sustained for all fields having arbitrary intensity. As an initial approximation, we assume that the probe field $|A_n^0|$ is weak while the pump field $|A_0^1|$ is of arbitrary strength. Next, the leading term ($m=1$, $m'=1$, $n=0$, $n'=0$) in (2.23), which yields an exact solution, is extracted from the sum so that

$$w^0/ZT_1=\left[Z+1T_1+4g^2|A_0^1|^2\Lambda_{00}^{11}(Z)+4g^2{\sum}'\Lambda_{nn'}^{mm'}(Z)A_n^{m*}A_{n'}^{m'}T(\Omega_n^m-\Omega_{n'}^{m'})\right]w(Z)\ , \tag{2.25}$$

where the prime on the summation denotes that the leading term of the sum ($m=m'=1$) is omitted. Equation (2.25) now has the form

$$[a(Z)+T]w(Z)=f(Z)\ , \tag{2.26}$$

or equivalently we can invert the transformation to obtain

$$w(Z)=(1+a^{-1}T)^{-1}a^{-1}f(Z)\ . \tag{2.27}$$

A perturbation expansion of $(1+a^{-1}T)^{-1}$ in powers of the smaller terms $A_n^{m*}A_{n'}^{m'}$ of (2.25) where $m, m'\neq 1$ yields

$$\begin{aligned}w(Z)=\frac{w^0}{T_1}&\left[1-4g^2[Z+1/T_1+4g^2|A_0^1|^2\Lambda_{00}^{11}(Z)]^{-1}\sum_{\{n,m\}}{}'A_{n'}^{m'*}A_{n''}^{m''}\Lambda_{n'n''}^{m'm''}(Z)T(\Omega_{n'}^{m'}-\Omega_{n''}^{m''})\right]\\&\times Z^{-1}[Z+1/T_1+4g^2|A_0^1|^2\Lambda_{00}^{11}(Z)]^{-1}\ ,\end{aligned} \tag{2.28}$$

where the translation operator T operates on all terms to the right of it that depend on Z. The leading term of (2.28),

$$w(Z)=\frac{w^0}{T_1}\frac{1}{Z}\left[Z+\frac{1}{T_1}+4g^2|A_0^1|^2\Lambda_{00}^{11}(Z)\right]^{-1}\ , \tag{2.29}$$

which we now consider, generates a result equivalent to the rate equations. The remaining higher order $\sum'$ terms of (2.28), the coherence terms, modulate the population at the sideband frequencies $\Omega_{n'}^{m'}-\Omega_{n''}^{m''}$ and will be treated later as a correction. With the aid of (2.19a) and (2.29), we have

$$\tilde{\rho}_{12}(Z)=-\frac{2igw^0/T_1}{Z-i\Delta+1/T_2}\sum_{n,m}A_n^m(Z-i\Omega_n^m)^{-1}\left[Z-i\Omega_n^m+\frac{1}{T_1}+4g^2|A_0^1|^2\Lambda_{00}^{11}(Z-i\Omega_n^m)\right]^{-1}. \tag{2.30}$$

The inverse Laplace transform (2.18) applied to (2.30) yields

$$\tilde{\rho}_{12}(t)=-\sum_l\left[\frac{2igw^0/T_1}{i(l\Omega-\Delta)+1/T_2}\right]\left[\frac{A_l^0e^{il\Omega t}}{1/T_1+4g^2|A_0^1|^2\Lambda_{00}^{11}(0)}\right], \tag{2.31}$$

where we have considered only the poles $Z=in\Omega$ as the others, with decay time T_2 or shorter, are strongly damped in the long time limit $t>>T_2$.

Notice that $\tilde{\rho}_{12}$ generates the signal field (2.14)

$$\tilde{E}_s^+(z',t)=\sum_l D_le^{il\Omega t}, \tag{2.32}$$

where

$$D_l=\frac{-8ig^4(T_1/T_2)w^0|A_0^1|^2A_l^0}{\Delta-l\Omega+i/T_2}\left[(\Delta-2kv_z)^2+\frac{1}{T_2^2}+4g^2(T_1/T_2)|A_0^1|^2\right]^{-1}, \tag{2.33}$$

and we have omitted the unsaturated term anticipating that it vanishes upon Doppler integration. To this order of approximation, $\tilde{E}_s^+$ is emitted in the direction of the probe beam as the above term $D_l \rightsquigarrow A_l^0=\tilde{E}_0e^{-ikz'}a_l$ indicates.

The heterodyne beat signal (2.16) then follows from the signal field (2.32) and the probe field (2.7) with $m=0$ where

$$B(t)=\sum_{n,l}A_n^0e^{in\Omega t}D_l^*e^{-il\Omega t}+\text{c.c.} \tag{2.34}$$

Selecting those terms in the double sum which give the fundamental beat term $E^{\pm i\Omega t}$, we find that

$$B(t)=\sum_l[A_{l-1}^*A_lf(l)+A_{l+1}A_l^*f^*(l)]e^{i\Omega t}+\text{c.c.}, \tag{2.35}$$

where $f(l)$ consists of the remaining terms of D_l. The relations (2.3b) allow us to prove that the index interchange $l\rightarrow -l$ results in

$$A_{l+1}A_l^*\rightarrow -A_{l-1}^*A_l, \tag{2.36}$$

and thus the terms can be combined as

$$B(t)=\sum_l A_{l-1}^*A_l[f(l)-f^*(-l)]e^{i\Omega t}+\text{c.c.} \tag{2.37}$$

or

$$B_0(t)=\frac{-8ig^4(T_1/T_2)w^0|A_0^1|^2}{(\Delta-2kv_z)^2+1/T_2^2+4g^2(T_1/T_2)|A_0^1|^2}\times\sum_l A_{l-1}^*A_l\left[\frac{1}{\Delta-l\Omega+i/T_2}+\frac{1}{\Delta+l\Omega-i/T_2}\right]+\text{c.c.} \tag{2.38}$$

The Doppler integral (2.15) of $B(t)$ can be carried out by contour integration to give a result equivalent to that of the rate equations,

$$\langle B_0(t)\rangle=-8i\pi Ng^4w^0|A_0^1|^2\frac{T_1}{T_2}\frac{e^{i\Omega t}}{\alpha}\sum_l A_{l-1}^*A_l\delta\frac{\delta^1-(l\Omega/2)^2+\Gamma^2-i\Gamma l\Omega}{\left[\left[\delta-\frac{l\Omega}{2}\right]^2+\Gamma^2\right]\left[\left[\delta+\frac{l\Omega}{2}\right]^2+\Gamma^2\right]}+\text{c.c.} \tag{2.39}$$

with

$$\alpha=\frac{1}{T_2}(1+4g^2T_1T_2|A_0^1|^2)^{1/2}\ , \tag{2.40}$$

$$\Gamma=\tfrac{1}{2}(\alpha+1/T_2)\ , \tag{2.41}$$

$$\delta=\omega_{21}-\omega_0\ , \tag{2.42}$$

and $N=1/(\sqrt{\pi}ku)$ is the normalization factor of (2.15).

The behavior of (2.39) is easily seen by considering only the central component with $l=0$ and the two sidebands at $\omega_0\pm\Omega$ with $l=+1$, which yields

$$\langle B_0(t)\rangle = -16\pi Ng^4\tilde{E}_0^2\tilde{E}_1^2w^0\frac{T_1}{T_2}\frac{J_0(M)J_1(M)}{\alpha}\delta\left[\left[\frac{1}{\delta^2+\Gamma^2}-\frac{\delta^2-(\Omega/2)^2+\Gamma^2}{\left[\left[\delta-\frac{\Omega}{2}\right]^2+\Gamma^2\right]\left[\left[\delta+\frac{\Omega}{2}\right]^2+\Gamma^2\right]}\right]\cos\Omega t - \frac{\Gamma\Omega}{\left[\left[\delta-\frac{\Omega}{2}\right]^2+\Gamma^2\right]\left[\left[\delta+\frac{\Omega}{2}\right]^2+\Gamma^2\right]}\sin\Omega t\right]\ . \tag{2.43}$$

Equation (2.43) displays dispersive (in-phase) and absorptive (out-of-phase) power-broadened Lorentzian line shapes of width Γ as shown in Fig. 1. The central resonance $\omega_{21}=\omega_0$, which occurs when the laser is tuned to the peak of the Doppler line shape, is purely dispersive. To understand the sideband resonance $\omega_0=\omega_{21}-\Omega/2$, note that the pump must burn a hole in a packet shifted from the Doppler peak by $\Omega/2$ in order that the counterpropagating high-frequency sideband at $\omega_{21}+\Omega/2$ can come into resonance with the same packet. Similarly, the resonance at $\omega_0=\omega_{21}+\Omega/2$ occurs when the pump is displaced by $-\Omega/2$ from the Doppler peak. In contrast to the central feature, the sidebands show both absorptive and dispersive line shapes, the latter being opposite in sign from the central line.

Consideration of other terms in (2.39) results in a correction of (2.43) as well as higher-order resonances at

$$\delta=\pm\frac{l\Omega}{2}\ .$$

Finally, the rate equations predict a beat signal only in the forward direction, the direction of the probe beam, as indicated by the $e^{-ikz'}$ factor contained in the signal field (2.33).

The absence of a beat in the backward direction is easily understood, as the rate-equation approximation completely neglects the coherent oscillations of the population. Therefore, the backward travelling pump remains a single frequency field which is incapable of producing a heterodyne beat. In Sec. II E, this case is treated.

Finally, an experimental situation might arise where both the forward and backward waves are phase modulated. A similar calculation to the above reveals that

$$\langle B(t)\rangle = -8i\pi Ng^4w^0T_1\sum_{mn'}|A_{n'}^1|^2A_{n-1}^{0*}A_ne^{i\Omega t}\times\delta\frac{\delta^2+1/T_2^2-\left[\frac{n-n'}{2}\Omega\right]^2-i(n-n')\frac{\Omega}{T_2}}{\left\{\left[\delta-\left[\frac{n-n'}{2}\Omega\right]\right]^2+1/T_2^2\right\}\left[\left[\delta+\frac{n-n'}{2}\Omega\right]^2+1/T_2^2\right]}+\text{c.c.}\ ,$$

which resembles (2.39).

D. Coherence effects

The rate-equation result (2.39) ignores coherence effects, i.e., sideband terms that coherently modulate the population at frequency $n\Omega$. When coherence is included, beat signals appear in both forward and backward directions and new resonances are found. We therefore return to (2.28) and consider for the moment only those terms omitted in the rate-equation calculation. With (2.28) and (2.22a), we now obtain

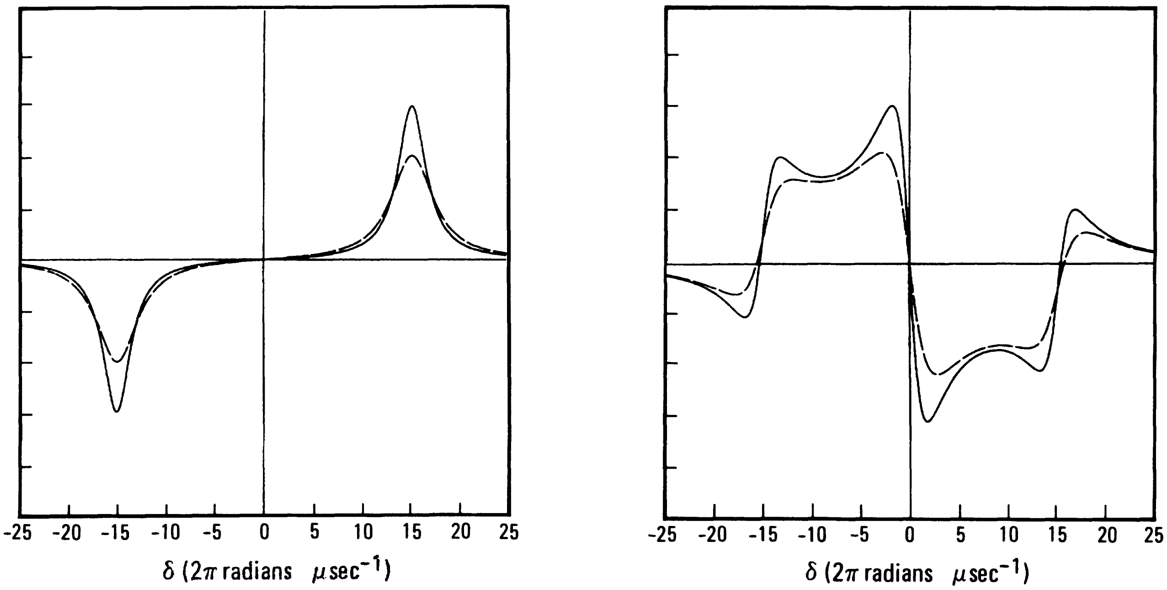

FIG. 1. Theoretical absorption (left) and dispersion (right) line shapes for a two-level atom interacting simultaneously with a pump field and a counterpropagating phase-modulated probe field which is detected. The frequency axis $\delta=\omega_{21}-\omega_0$. Solid curve: Eq. (2.55) which is equivalent to a rate-equation result. Dashed curve: the sum of (2.55) and the coherence correction (2.56). Parameters: $T_2=1$ μsec, $x=5$, $\Omega=30$ (2π radiansμsec^{-1}), and $\overline{\Gamma}=1.72$.

$$\tilde{\rho}_{12}(Z)=\frac{8ig^3w^0/T_1}{Z-i\Delta+1/T_2}\sum_{n,m}{}' A_n^m[Z-i\Omega_n^m+1/T_1+4g^2|A_0^1|^2\Lambda_{00}^{11}(Z-i\Omega_n^m)]^{-1}$$
$$\times \sum_{\{n',m'\}}{}' A_{n'}^{m'*}A_{n''}^{m''}\Lambda_{n',n''}^{m',m''}(Z-i\Omega_n^m)T(\Omega_{n'}^{m'}-\Omega_{n''}^{m''}-\Omega_n^m)$$
$$\times\frac{1}{Z}\left[Z+\frac{1}{T_1}+4g^2|A_0^1|^2\Lambda_{00}^{11}(Z)\right]^{-1}. \tag{2.44}$$

In anticipating the Laplace transform, we first notice that $T(\Omega_{n'}^{m'}-\Omega_{n''}^{m''}-\Omega_n^m)/Z$ provides the only pole that is not damped in the long-time limit. Secondly, our interest is restricted to terms that oscillate at $l\Omega$ so that in (2.44) the operator $T=T(-l\Omega)$. Thirdly, the amplitude product $A_n^mA_{n'}^{m'*}A_{n''}^{m''}$ contains the phase factors

$$e^{i(k^m-k^{m'}+k^{m''})z'},$$

where

$$k^m=\begin{cases} k & m=1, \\ -k & m=0, \end{cases} \tag{2.45}$$

as indicated in (2.5) and (2.6). Eight possible combinations of the values exist, but only three are relevant:

$$m=1,\ m'=1,\ m''=0 \Longrightarrow e^{-ikz'}, \tag{2.46a}$$

$$m=1,\ m'=0,\ m''=0 \Longrightarrow e^{ikz'}, \tag{2.46b}$$

$$m=0,\ m'=0,\ m''=1 \Longrightarrow e^{ikz'}, \tag{2.46c}$$

where $m=1 \Longrightarrow n=0$ and $m=0 \Longrightarrow n=\pm 1, \pm 2, \ldots$. Considering the case (2.46a) where the signal field propagates in the direction of the probe beam, the Laplace transform of (2.44) evaluated at the pole $Z=il\Omega$ gives the signal field $\tilde{E}_s^+$, (2.32), where

$$D_l=\frac{-8ig^4w^0}{\Delta-l\Omega+i/T_2}|A_0^1|^2A_l^0[il\Omega-i2kv_z+1/T_1+4g^2|A_0^1|^2\Lambda_{00}^{11}(il\Omega-i2kv_z)]^{-1}$$
$$\times\Lambda_{0l}^{10}(il\Omega-i2kv_z)\left[1+4g^2|A_0^1|^2\frac{T_1}{T_2}\frac{1}{(\delta-kv_z)^2+1/T_2^2}\right]^{-1}. \tag{2.47}$$

Notice that the Doppler integral of (2.47) vanishes when the $|A_0^1|^2$ term of the last line of (2.47) is neglected. This observation causes us to rewrite the last, large-parentheses expression as

$$[\;]^{-1}=1-\frac{4g^2|A_0^1|^2T_1/T_2}{(\delta-kv_z)^2+1/T_2^2+4g^2|A_0^1|^2T_1/T_2}. \tag{2.48}$$

Equation (2.47) then becomes

$$D_l=\frac{32ig^6(T_1/T_2)w^0|A_0^1|^4A_l^0}{\Delta-l\Omega+i/T_2}\Lambda_{0l}^{10}(il\Omega-i2kv_z)$$
$$\times[il\Omega-i2kv_z+1/T_1+4g^2|A_0^1|^2\Lambda_{00}^{11}(il\Omega-i2kv_z)]^{-1}$$
$$\times[(\delta-kv_z)^2+1/T_2^2+4g^2|A_0^1|^2T_1/T_2]^{-1}. \tag{2.49}$$

The remaining steps follow the rate-equation calculation.

The coherence correction to the heterodyne beat signal (2.37) takes the form

$$B_1(t)=\frac{32g^6(T_1/T_2)w^0e^{i\Omega t}|A_0^1|^4}{(\delta-kv_z)^2+1/T_2^2+4g^2|A_0^1|^2T_1/T_2}$$
$$\times\sum_l A_{l-1}^*A_l\left[\frac{\Lambda_{0l}^{10}(il\Omega-i2kv_z)}{\Delta-l\Omega+i/T_2}\left[-l\Omega+2kv_z+\frac{i}{T_1}+4ig^2|A_0^1|^2\Lambda_{00}^{11}(il\Omega-2ikv_z)\right]^{-1}-(l\to-l)^*\right]+\text{c.c.}, \tag{2.50}$$

where

$$\Lambda_{0l}^{10}(il\Omega-i2kv_z)=\frac{i}{2}\left[\frac{1}{-l\Omega+\Delta+i/T_2}+\frac{1}{kv_z-\delta+i/T_2}\right],$$
$$\Lambda_{00}^{11}(il\Omega-i2kv_z)=\frac{i}{2}\left[\frac{1}{-l\Omega+\Delta+i/T_2}+\frac{1}{-l\Omega+3kv_z-\delta+i/T_2}\right]. \tag{2.51}$$

The appearance of $2kv_z$ and $3kv_z$ in the above resonance denominators suggests higher-order resonances. However, these effects disappear on Doppler integration and would be observed only in the presence of a third field as witnessed in previous studies.[12,13]

By contour integration, the Doppler integral of $B_1(t)$ is

$$\langle B_1(t)\rangle=-\frac{2\pi}{\Gamma\alpha}Ng^6w^0\frac{T_1}{T_2}|A_0^1|^4e^{i\Omega t}$$
$$\times\sum_l A_{l-1}^*A_l\left\{\left[\frac{\delta-l\Omega/2+2i\Gamma}{\delta-l\Omega/2+i\Gamma}\right](\delta-l\Omega/2+i\Gamma+i\alpha)\right.$$
$$\times\left[\left[-\frac{l\Omega}{2}+\delta+i\alpha+i/2T_1\right]\left[\delta-\frac{l\Omega}{2}+i\Gamma\right]\left[\delta-\frac{l\Omega}{2}+i\alpha+i\Gamma\right]\right.$$
$$\left.\left.-g^2|A_0^1|^2\left[\delta-\frac{l\Omega}{2}+i\Gamma+i\alpha/2\right]\right]^{-1}-\text{c.c.}(l\to-l)\right\}+\text{c.c.} \tag{2.52}$$

The final result is the sum of (2.39) and (2.52),

$$\langle B(t)\rangle=\langle B_0(t)+B_1(t)\rangle \;. \tag{2.53}$$

Let us treat the case $l=0$ and $l=+1$ again using the reduced variables and definitions

$$\begin{aligned} &x=4g^2T_1T_2\,|A_0^1|^2,\quad \bar{\alpha}=\sqrt{1+x}\;,\\ &\bar{\Gamma}=\tfrac{1}{2}(1+\sqrt{1+x}\,),\quad T_2=2T_1\;,\\ &\bar{\Omega}=T_2\Omega,\quad \bar{\delta}=T_2\delta\;. \end{aligned} \tag{2.54}$$

We find

$$\langle B_0\rangle=-2\bar{\delta}\frac{x}{\sqrt{1+x}}\left[\frac{\bar{\Gamma}\bar{\Omega}+i[\bar{\delta}^2+\bar{\Gamma}^2-(\bar{\Omega}/2)^2]}{[(\bar{\delta}-\bar{\Omega}/2)^2+\bar{\Gamma}^2][(\bar{\delta}+\bar{\Omega}/2)^2+\bar{\Gamma}^2]}-\frac{i}{\bar{\delta}^2+\bar{\Gamma}^2}\right], \tag{2.55}$$

and

$$\langle B_1\rangle=-\frac{1}{2}\frac{x^2}{\sqrt{1+x}\,(1+\sqrt{1+x})}[F(\bar{\Omega})-F^*(-\bar{\Omega})-F(0)+F^*(0)]\;,$$

where

$$\begin{aligned} F(\bar{\Omega})=\;&\frac{\bar{\delta}-\dfrac{\bar{\Omega}}{2}+2i\bar{\Gamma}}{\bar{\delta}-\dfrac{\bar{\Omega}}{2}+i\bar{\Gamma}}\left[\bar{\delta}-\frac{\bar{\Omega}}{2}+i\bar{\Gamma}+i\bar{\alpha}\right]\\ &\times\left[\left[\bar{\delta}-\frac{\bar{\Omega}}{2}+i\bar{\Gamma}\right]\left[\bar{\delta}-\frac{\bar{\Omega}}{2}+i\bar{\Gamma}+i\bar{\alpha}\right]\left[\bar{\delta}-\frac{\bar{\Omega}}{2}+i\bar{\alpha}+i\right]-\tfrac{1}{2}\left[\bar{\delta}-\frac{\bar{\Omega}}{2}+i\bar{\Gamma}+i\frac{\bar{\alpha}}{2}\right]\right]^{-1}\;. \end{aligned} \tag{2.56}$$

The coherence correction $\langle B_1\rangle$ to the rate-equation result $\langle B_0\rangle$ is illustrated in Fig. 1 and is reminiscent of Lamb-dip theories[14(a)] when coherence contributions are included.

For weak fields, the ratio of the coherence correction to the rate-equation contribution is

$$\frac{\langle B_1\rangle}{\langle B_0\rangle}\sim\frac{T_2}{T_1}4g^2T_1T_2\,|A_0^1|^2\;.$$

Thus, the rate equations are valid only when $T_2<<T_1$ and the fields are weak,

$$4g^2T_1T_2\,|A_0^1|^2<<1\;.$$

E. The backward wave

Now consider beat signals that propagate in the backward direction, the direction of the pump field. Analysis shows that case (2.46c) is qualitatively similar to the coherence correction of the beat signal propagating in the forward direction (2.46a) and is of higher order, being proportional to $|A_0^1|^4$. The dominant beat signal in the backward direction corresponds to (2.46b) which we now discuss in detail. The starting point is (2.44) and takes the form

$$\begin{aligned} \tilde{\rho}_{12}(Z)=\;&\frac{8ig^3w^0/T_1}{Z-i\Delta+1/T_2}\sum_{n',n''}{}'A_0^1A_{n'}^{0*}A_{n''}^0\\ &\times[Z-2ikv_z+1/T_1+4g^2|A_0^1|^2\Lambda_{00}^{11}(Z-i2kv_z)]^{-1}\\ &\times\Lambda_{n'n''}^{00}(Z-2ikv_z)\{Z-i[2kv_z-\Omega(n'-n'')]\}^{-1}\\ &\times\{Z-i[2kv_z-\Omega(n'-n'')]+1/T_1\\ &\quad+4g^2|A_0^1|^2\Lambda_{00}^{11}[Z-i(2kv_z-\Omega n'+\Omega n'')]\}^{-1} \end{aligned} \tag{2.57}$$

under the condition (2.46b).

To the lowest order of approximation, we drop the power broadening $|A_0^1|^2$ terms in the above denominators and perform the Laplace transform at the pole $Z=2ikv_z-i\Omega(n'-n'')$ to obtain

$$\tilde{\rho}_{12}(t)=-4g^3w^0A_0^1\sum_{n',n''}A_{n'}^{0*}A_{n''}^{0}\frac{1}{\Omega(n'-n'')+i/T_1}e^{2ikv_zt-i(n'-n'')\Omega t}$$
$$\times[kv_z-\delta-(n'-n'')\Omega-i/T_2]^{-1}$$
$$\times[(kv_z+\delta-n''\Omega+i/T_2)^{-1}-(kv_z+\delta-n'\Omega-i/T_2)^{-1}]\ . \tag{2.58}$$

Proceeding as in Sec. II C, the signal field

$$\tilde{E}_s^+\sim ig\tilde{\rho}_{12}$$

appears in the heterodyne beat expression

$$B(t)=\tilde{E}^+\tilde{E}_s^-+\tilde{E}^-\tilde{E}_s^+\ , \tag{2.59}$$

where we see that the pump field

$$\tilde{E}^+(t)=A_0^1e^{2ikv_zt}$$

cancels the e^{2ikv_zt} factor of (2.58).

Upon Doppler integration of (2.59) and with the manipulations (2.35) and (2.36) to extract beats oscillating at $e^{i\Omega t}$, we find that

$$\langle B(t)\rangle=-8\pi g^4w^0N\frac{T_1}{[1+(\Omega T_1)^2]^{1/2}}|A_0^1|^2e^{i(\Omega t+\varphi)}$$
$$\times\sum_l A_{l-1}^*A_l\delta\frac{\delta^2-\left[\dfrac{\Omega}{2}(l+1)\right]^2+1/T_2^2+i\dfrac{\Omega(l+1)}{T_2}}{\left[\left[\delta-\dfrac{\Omega}{2}(l+1)\right]^2+1/T_2^2\right]\left[\left[\delta+\dfrac{\Omega}{2}(l+1)\right]^2+1/T_2^2\right]}+\text{c.c.}\ , \tag{2.60}$$

where $\tan\varphi=1/(\Omega T_1)$. To see the behavior of (2.60) in lowest order, we again select terms in $l=0$ and $l=+1$ with the result

$$\langle B(t)\rangle=-16\pi g^4w^0N\frac{T_1}{[1+(\Omega T_1)^2]^{1/2}}\tilde{E}_0^2\tilde{E}_1^2J_0(M)J_1(M)$$
$$\times\delta\left[\left[\frac{\Omega/T_2}{\left[\left[\delta-\dfrac{\Omega}{2}\right]^2+1/T_2^2\right]\left[\left[\delta+\dfrac{\Omega}{2}\right]^2+1/T_2^2\right]}-\frac{2\Omega/T_2}{[(\delta-\Omega)^2+1/T_2^2][(\delta+\Omega)^2+1/T_2^2]}\right]\cos(\Omega t+\varphi)\right.$$
$$\left.+\left[\frac{\delta^2-(\Omega/2)^2+1/T_2^2}{\left[\left[\delta-\dfrac{\Omega}{2}\right]^2+1/T_2^2\right]\left[\left[\delta+\dfrac{\Omega}{2}\right]^2+1/T_2^2\right]}-\frac{\delta^2-\Omega^2+1/T_2^2}{[(\delta-\Omega)^2+1/T_2^2][(\delta+\Omega)^2+1/T_2^2]}\right]\sin(\Omega t+\varphi)\right]\ . \tag{2.61}$$

Thus, the backward wave displays Lorentzian line shapes of width $1/T_2$ in absorption and dispersion when the resonance conditions $\delta=\pm\Omega/2$ and $\delta=\pm\Omega$ are satisfied. A plot of (2.61) in Fig. 2 reveals that the $\Omega/2$ and Ω resonances are of opposite sign but are equal in absolute magnitude. Unlike the beat signal of the forward wave (2.43), the $\delta=\pm\Omega$ resonances are new and the $\delta=0$ resonance is missing. The beats expected in the forward direction have indeed been observed[1(b),3] and the prediction (2.61) has just been detected in this laboratory.[14(b)]

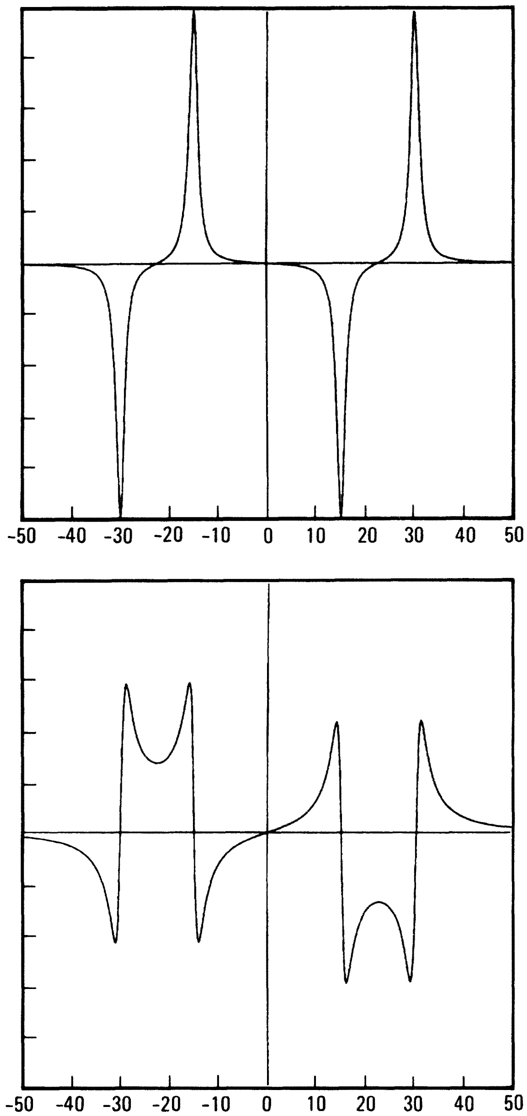

FIG. 2. Theoretical absorption (upper curve) and dispersion (lower curve) line shapes for a two-level atom interacting simultaneously with a pump field and a counterpropagating phase-modulated probe field, Eq. (2.61). In this case the pump beam is detected, and besides the $\delta=\pm\Omega/2$ resonances, new resonances appear at $\delta=\pm\Omega$ due to the inclusion of coherence corrections. Parameters: $T_2=1$ μsec and $\Omega=30$ (2π radians$\,\mu$sec^{-1}).

III. SOLIDS

A. Two-level problem

A number of hole-burning experiments have been reported recently in solid-state laser spectroscopy.[15] A pump field burns a hole which resides in the ground-state population distribution long after the field is removed. A weaker probe field then follows and monitors the memory of the hole in one or more transitions, revealing hyperfine structure and potentially dynamic line broadening effects. Since phase modulation is useful in this application,[16] we present the relevant theory.

The previous two-level formalism can be adopted except that the pump field

$$E_1(z,t)=\tilde{E}_1 e^{i(\Omega_1 t-k_1 z)}+\text{c.c.}\ , \tag{3.1}$$

which replaces (2.1), propagates in the same direction as the probe field (2.2),

$$E_2(z,t)=\tilde{E}_2 e^{i(\Omega_2 t-k_2 z)}e^{i\varphi(t)}+\text{c.c.}\ , \tag{3.2}$$

where the indices are changed for convenience, $k\equiv k_1\sim k_2$, $A_0^1=\tilde{E}_1 e^{-ikz'}$, and $\Omega_0^1=0$. Since the pump and probe occupy different time intervals, the treatment is significantly simpler than Sec. II. For the preparative stage, the equations of motion (2.8) are now

$$\frac{d\tilde{\rho}_{12}}{dt}=(i\Delta_1-1/T_2)\tilde{\rho}_{12}-2igw\tilde{E}_1\ , \tag{3.3a}$$

$$\dot{w}=-(w-w^0)/T_1-ig\tilde{E}_1(\tilde{\rho}_{12}-\tilde{\rho}_{21})\ , \tag{3.3b}$$

where

$$\Delta_i=\omega_{21}-\Omega_i+kv_z,\ \ i=1,\,2\ . \tag{3.4}$$

The steady-state solution, $d\tilde{\rho}_{12}/dt=\dot{w}=0$, is

$$w_{ss}=w^0\left[1-\frac{4g^2|\tilde{E}_1|^2T_1/T_2}{\Delta_1^2+1/T_2^2+4g^2|\tilde{E}_1|^2T_1/T_2}\right]. \tag{3.5}$$

For the probing stage, we obtain a perturbation solution of

$$\frac{d\rho_{12}}{dt}=(i\Delta_2-1/T_2)\tilde{\rho}_{12}-2igw_{ss}\sum_n A_n e^{in\Omega t} \tag{3.6}$$

in the long-time limit $t>>T_2$ with

$$\tilde{\rho}_{12}(t) = -2igw_{ss}\sum_n A_n e^{in\Omega t}(-i\Delta_2 + in\Omega + 1/T_2) , \tag{3.7}$$

w_{ss} being given by (3.5). Contour integration of the Doppler-like integral of $\tilde{\rho}_{12}(t)$ followed by the manipulations (2.35) and (2.36) yields the beat signal

$$\langle B(t)\rangle = -8i\pi w^0 N g^4 |\tilde{E}_1|^2 \frac{T_1}{T_2\alpha} e^{i\Omega t} \times \sum_l A_{l-1}^* A_l \delta' \frac{\delta'^2 - (l\Omega/2)^2 - i\Gamma l\Omega + \Gamma^2}{[(\delta' - l\Omega/2)^2 + \Gamma^2][(\delta' + l\Omega/2)^2 + \Gamma^2]} + \text{c.c.} , \tag{3.8}$$

where

$$\delta' = (\Omega_1 - \Omega_2)/2 ,$$

and α and Γ are defined by (2.40) and (2.41). This result has precisely the same form as the case of the counterpropagating pump and probe beams, Eq. (2.39), except that the tuning parameter changes from the off-resonance parameter $\delta = \omega_{21} - \omega_0$ to the laser frequency difference $\delta' = (\Omega_1 - \Omega_2)/2$. Hence, the beat signals will have the appearance of Fig. 1.

B. Three-level problem

In the spirit of the previous section, we now treat a three-level quantum system where two optical transitions, $1 \to 3$ and $1 \to 2$, share a common lower level. In the preparation the pump field (3.1) first excites one of the transitions, and thereafter, the probe field (3.2) samples the residual hole in the population distribution of level 1 in either transition. At first sight, it would appear that the three-level case offers nothing new. However, careful analysis shows that the two transitions, as seen by the probe, do not exhibit the same response.

For the preparative stage, the density-matrix equations of motion can be written as

$$\begin{aligned}
\frac{d\tilde{\rho}_{21}}{dt} &= i\Delta_{21}\tilde{\rho}_{21} - ig_1\tilde{E}_1^-(\rho_{11} - \rho_{22}) + ig_2\tilde{E}_1^-\rho_{23} - \Gamma\tilde{\rho}_{21} , \\
\frac{d\tilde{\rho}_{31}}{dt} &= i\Delta_{31}\tilde{\rho}_{31} - ig_2\tilde{E}_1^-(\rho_{11} - \rho_{33}) + ig_1\tilde{E}_1^-\rho_{32} - \Gamma\tilde{\rho}_{31} , \\
\frac{d\tilde{\rho}_{23}}{dt} &= i\Delta_{23}\tilde{\rho}_{23} - ig_1\tilde{E}_1^-\tilde{\rho}_{13} + ig_2\tilde{E}_1^+\tilde{\rho}_{21} - \Gamma'\rho_{23} , \\
\dot{\rho}_{11} &= \gamma_2\rho_{22} + \gamma_3\rho_{33} + ig_1(-\tilde{E}_1^+\tilde{\rho}_{21} + \tilde{E}_1^-\tilde{\rho}_{12}) + ig_2(-\tilde{E}_1^+\tilde{\rho}_{31} + \tilde{E}_1^-\tilde{\rho}_{13}) , \\
\dot{\rho}_{22} &= ig_1(-\tilde{E}_1^-\tilde{\rho}_{12} + \tilde{E}_1^+\tilde{\rho}_{21}) - \gamma_2\rho_{22} , \\
\dot{\rho}_{33} &= ig_2(-\tilde{E}_1^-\tilde{\rho}_{13} + \tilde{E}_1^+\tilde{\rho}_{31}) - \gamma_3\rho_{33} .
\end{aligned} \tag{3.9}$$

The following matrix elements and definitions apply:

$$\begin{aligned}
&H_{ii} = \hbar\omega_i, \quad \omega_{ij} = \omega_i - \omega_j, \quad i \text{ or } j = 1, 2, 3 \\
&H_{12} = g_1\hbar E_1, \quad H_{13} = g_2\hbar E_1, \quad H_{23} = 0 , \\
&\rho_{ij} = \tilde{\rho}_{ij} e^{i(\Omega_1 - kv_z)t}, \quad ij = 12 \text{ or } 13 \\
&\Delta_{21} = \Omega_1 - \omega_{21} - kv_z , \\
&\Delta_{31} = \Omega_1 - \omega_{31} - kv_z , \\
&\Delta_{23} = \omega_{32} .
\end{aligned} \tag{3.10}$$

We also assume that the system is isolated so that

$$1=\rho_{11}+\rho_{22}+\rho_{33} ,$$

and that the pump field resonantly excites one transition or the other, but not both simultaneously so that we expect that

$$\tilde{\rho}_{23}\sim 0 .$$

For simplicity, we assume that

$$g\equiv g_1=g_2 \text{ and } \gamma\equiv\gamma_2=\gamma_3 .$$

In steady state, the solutions are

$$w_{12}^{ss}=\frac{(\Delta_{31}^2+\Gamma^2)(\Delta_{21}^2+\Gamma^2)+a^2(\Delta_{21}^2+\Gamma^2)}{(\Delta_{31}^2+\Gamma^2)(\Delta_{21}^2+\Gamma^2)+2a^2(\Delta_{31}^2+\Delta_{21}^2+2\Gamma^2)+3a^4} , \tag{3.11}$$

$$w_{13}^{ss}=\frac{(\Delta_{21}^2+\Gamma^2)(\Delta_{31}^2+\Gamma^2)+a^2(\Delta_{31}^2+\Gamma^2)}{(\Delta_{31}^2+\Gamma^2)(\Delta_{21}^2+\Gamma^2)+2a^2(\Delta_{31}^2+\Delta_{21}^2+2\Gamma^2)+3a^4} , \tag{3.12}$$

where

$$a^2=\frac{2g^2}{\gamma}\Gamma\,|E_1|^2 .$$

For the probing period, lowest-order perturbation theory yields the equation of motion

$$\frac{d\tilde{\rho}_{21}}{dt}=i\bar{\Delta}_{21}\tilde{\rho}_{21}-ig\sum_n A_n^* e^{-in\Omega t}w_{12}^{ss}-\Gamma\tilde{\rho}_{21} ,$$

which has the long-time ($t>>T_2$) solution

$$\tilde{\rho}_{21}(t)=-ig\sum_n w_{12}^{ss}A_n^* e^{-in\Omega t}\frac{1}{-in\Omega-i\bar{\Delta}_{21}+\Gamma} .$$

Similarly,

$$\tilde{\rho}_{31}(t)=\tilde{\rho}_{21}(2\leftrightarrow 3) ,$$

where

$$\bar{\Delta}_{21}=\Omega_2-\omega_{21}-kv_z ,$$

$$\bar{\Delta}_{31}=\Omega_2-\omega_{31}-kv_z .$$

Proceeding as before, the signal field is

$$\tilde{E}_s^-\sim -ig(\tilde{\rho}_{21}+\tilde{\rho}_{31}) ,$$

and the heterodyne beat is of the form

$$B(t)=-g^2\sum_l e^{i\Omega t}A_{l+1}A_l^* \times\left[\frac{w_{12}^{ss}}{-il\Omega-i\bar{\Delta}_{21}+\Gamma}-\frac{w_{12}^{ss}}{-il\Omega+i\bar{\Delta}_{21}+\Gamma}+\frac{w_{13}^{ss}}{-il\Omega-\bar{\Delta}_{31}+\Gamma}-\frac{w_{13}^{ss}}{-il\Omega+i\bar{\Delta}_{31}+\Gamma}\right] . \tag{3.13}$$

To carry out the Doppler integration, we consider the weak-field case

$$w_{12}^{ss}=1-a^2\frac{(\Delta_{21}^2+\Gamma^2)+2(\Delta_{31}^2+\Gamma^2)}{(\Delta_{31}^2+\Gamma^2)(\Delta_{21}^2+\Gamma^2)} ,$$

$$w_{13}^{ss}=(w_{12}^{ss})(2\leftrightarrow 3) , \tag{3.14}$$

where power broadening is ignored by neglecting the a^2 and a^4 terms in the denominators of (3.11) and (3.12).

Upon the Doppler-like integration of (3.13), the final result is

$$\langle B(t)\rangle = 4\pi i \frac{g^4 |E_1|^2}{\gamma} e^{i\Omega t} \sum_l A_{l+1} A_l^* \, [4F_l(\Delta)+F_l(\Delta-\delta)+F_l(\Delta+\delta)] + \text{c.c.} \tag{3.15}$$

with

$$F_l(\Delta)=\Delta \frac{-(l\Omega)^2+\Delta^2+4\Gamma^2+4i\Gamma l\Omega}{[(l\Omega+\Delta)^2+4\Gamma^2][(l\Omega-\Delta)^2+4\Gamma^2]},$$

$$\Delta=\Omega_2-\Omega_1,$$

$$\delta=\omega_{23}.$$

Equation (3.15) is shown in Fig. 3 for the case $l=0$ and $l=-1$ and shares common features with the copropagating beam two-level case (3.8). The dispersion spectrum consists of a central triplet feature at $\Omega_2=\Omega_1$ and $\Omega_2=\Omega_1\pm\omega_{23}$, while one sideband appears as a triplet at $\Omega_2=\Omega_1-\Omega$ and $\Omega_2=\Omega_1-\Omega\pm\omega_{23}$ and the other sideband at $\Omega_2=\Omega_1+\Omega$ and $\Omega_2=\Omega_1+\Omega\ \pm\omega_{23}$. The absorption shows two triplets centered at $\Omega_2=\Omega_1\pm\Omega$, corresponding to the dispersion spectrum, but now the central feature is missing as in the two-level case of Fig. 1. Also, the Lorentzian line shape has a width of 2Γ due to the separate contributions of pump and probe absorption.

Note that the central absorption components at $\Omega_2=\Omega_1\ \pm\Omega$ are four times as intense as the satellite lines at $\Omega_2=\Omega_1\pm\Omega\pm\omega_{23}$. Two factors contribute to this ratio. First, the central component is due to two transitions, $1\rightarrow3$ and $1\rightarrow2$, which are excited at the same frequency due to the inhomogeneous broadening whereas the satellite lines are single transitions. This effect contributes a factor of 2. Second, the nonlinear response of a transition is proportional to the incremental change in population [see Eq. (2.8a)]. If the population change arising from hole burning is $-\delta$ for the lower state and $+\delta$ for the upper state, the central component intensity will be proportional to 2δ. However, the satellite line involves a common lower state with its contribution of $+\delta$ while the excited state is not prepared and therefore does not contribute. This effect provides the remaining factor of 2.

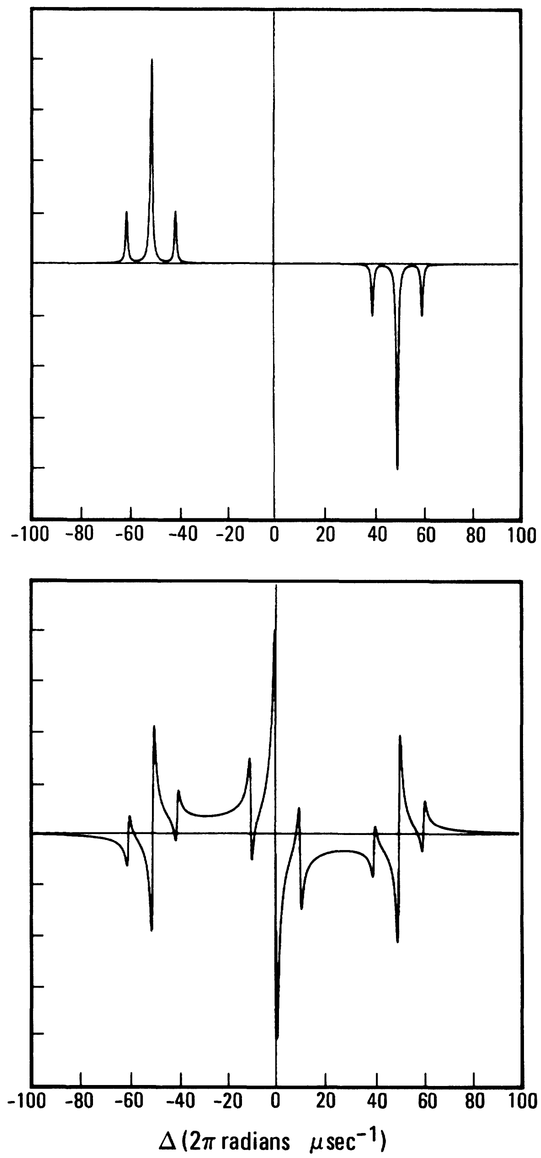

FIG. 3. Theoretical absorption (upper curves) and dispersion (lower curve) line shapes for a three-level atom interacting initially with a pump field of frequency Ω_1 and subsequently with a probe field of frequency Ω_2, Eq. (3.15). The frequency axis $\Delta=\Omega_2-\Omega_1$. Triplet features appear where the central line is four times the intensity of either satellite line. Parameters: $\Omega=50$ (2π radians μsec^{-1}), $\Gamma=0.25$ μsec^{-1}, and $\omega_{23}=10$ (2π radians μsec^{-1}).

IV. FABRY-PEROT

We now calculate the response of a plane mirror Fabry-Perot cavity to a phase-modulated laser beam. This linear problem, which contrasts with the nonlinear atomic case, is the basis of an important method for precision laser frequency (phase) locking.[2-4]

The incident field, which strikes the mirrors at normal incidence, is again given by (2.2), and the transmitted and reflected field amplitudes are well known[17] to be

$$E_t=\frac{1-R}{1-Re^{i\delta}}E_0\ , \tag{4.1}$$

$$E_r=\sqrt{R}\,\frac{1-e^{i\delta}}{1-Re^{i\delta}}E_0\ , \tag{4.2}$$

where R is the mirror's reflectivity and the phase change for a double traversal of a cavity of spacing d is

$$\delta=2nd\omega_0/c\ . \tag{4.3}$$

For a high-reflectivity cavity satisfying the condition $1-R<<1$, we approximate the phase factor by

$$e^{i\delta}\sim 1+i\delta\ . \tag{4.4}$$

Recognizing that the cavity resonance condition is

$$\delta_r=2nd\omega_r/c=m\,2\pi\quad (m=0,1,2,\ldots)\ , \tag{4.5}$$

we rewrite (4.4) as

$$e^{i\delta}=e^{i(\delta-\delta_r)}\sim 1+i\,2nd\Delta/c\ , \tag{4.6}$$

where the tuning parameter

$$\Delta=\omega_0-\omega_r\ . \tag{4.7}$$

Substitution of (4.6) into (4.1) and (4.2) gives

$$E_t=\frac{\Gamma(\Gamma+i\Delta)}{\Delta^2+\Gamma^2}E_0\ , \tag{4.8}$$

$$E_r=\frac{\Delta(\Delta-i\Gamma)}{\sqrt{R}\,(\Delta^2+\Gamma^2)}E_0\ , \tag{4.9}$$

with the linewidth defined by

$$\Gamma=\left[\frac{1-R}{R}\right]\left[\frac{c}{2nd}\right]\ .$$

The transmitted intensity then assumes the form

$$|E_t|^2=\Gamma^2\sum_l A^*_{l-1}A_l e^{i\Omega t}\left[\frac{\Gamma+i\Delta_l}{\Gamma^2+\Delta_l^2}\right]\times\left[\frac{\Gamma-i\Delta_{l-1}}{\Gamma^2+\Delta_{l-1}^2}\right]+\text{c.c.}\ , \tag{4.10}$$

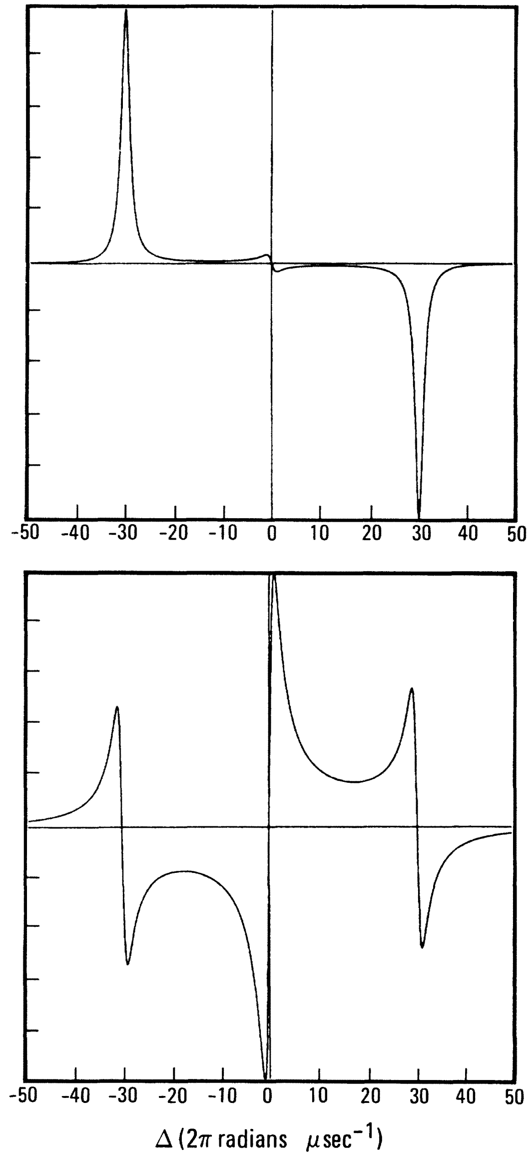

FIG. 4. Theoretical absorption (upper curve) and dispersion (lower curve) line shapes for a Fabry-Perot cavity subjected to a phase-modulated laser beam where detection is in reflection, Eq. (4.12). The frequency axis $\Delta=\omega_0-\omega_r$. The transmission line shape simply reverses sign as (4.13) indicates. Parameters: $\Omega=30$ (2π radiansμsec^{-1}), and $\Gamma=1$ μsec^{-1}.

where E_0 has been expanded into its sidebands through (2.3a) and we have retained in the sum only the beat terms containing $e^{i\Omega t}$. For the case $l=0$ and $l=+1$, Eq. (4.10) reduces to

$$|E_t|^2=-2\Omega\Gamma^2A_0A_1e^{i\Omega t}\,\Delta\frac{\Gamma^2+\Delta^2-\Omega^2+2i\Gamma\Omega}{(\Gamma^2+\Delta^2)[\Gamma^2+(\Delta+\Omega)^2][\Gamma^2+(\Delta-\Omega)^2]}+\text{c.c.} \tag{4.11}$$

Thus, three linear resonances appear (Fig. 4) at $\omega_0=\omega_r$ and $\omega_0=\omega_r\pm\Omega$, both in absorption and dispersion. In contrast to the nonlinear atomic response, (2.43) for example, the central line provides a nonvanishing absorption signal, an effect which apparently has gone unnoticed.[1-3] This central feature can disappear, however, when the absorption spectrum is not pure and contains a dispersive component when the phase angle θ is given by

$$\tan\theta=\frac{\Gamma^2-\Omega^2}{2\Gamma\Omega}\ .$$

A similar calculation for the intensity of the reflected component shows that

$$|E_r|^2=\frac{2\Omega}{R}A_0A_1e^{i\Omega t}\,\Delta\frac{i\Omega\Gamma(\Gamma^2-\Delta^2+\Omega^2)+\Gamma^2(\Gamma^2+\Delta^2+\Omega^2)}{(\Gamma^2+\Delta^2)[\Gamma^2+(\Delta+\Omega)^2][\Gamma^2+(\Delta-\Omega)^2]}+\text{c.c.}\ , \tag{4.12}$$

where we see that (4.11) and (4.12) are related by

$$|E_r|^2=-\frac{2}{R}\cos\phi(\Omega^2/\Gamma^2+1)^{1/2}|E_t|^2 \tag{4.13}$$

and $\tan\phi=\Omega/\Gamma$.

V. CONCLUSIONS

Calculations for several different cases that arise in phase-modulation laser spectroscopy have been developed. Various predictions are made including the role of higher-order coherence effects and the appearance of new resonances.

ACKNOWLEDGMENTS

We are pleased to acknowledge enlightening conversations with G. C. Bjorklund, S. A. Lee, J. L. Hall, R. W. P. Drever, and M. Levenson. This work was supported in part by the U. S. Office of Naval Research.

*On leave from the Department of Physics, Universität Essen, Gesamthochschule, Essen, West Germany.

[1](a) G. C. Bjorklund, Opt. Lett. 5, 15 (1980); (b) G. C. Bjorklund and M. D. Levenson, Phys. Rev. A 24, 166 (1981); (c) G. C. Bjorklund, K. Jain, and J. D. Hope, Appl. Phys. Lett. 38, 747 (1981).

[2]R. W. P. Drever, J. L. Hall, F. V. Kowalski, J. Hough, G. M. Ford, and A. Munley (unpublished); R. G. DeVoe and R. G. Brewer (unpublished).

[3]J. L. Hall, L. Hollberg, T. Baer, and H. G. Robinson, Appl. Phys. Lett. 39, 680 (1981).

[4]G. A. Sanders, M. G. Prentiss, and S. Ezekiel, Opt. Lett. 6, 569 (1981).

[5]R. W. P. Drever *et al.*, in *Laser Spectroscopy V,* Proceedings of the Fifth International Laser Spectroscopy Conference, Jasper, Canada, 1981, edited by A. R. W. McKellar, T. Oka, and B. P. Stoicheff (Springer, Berlin, 1981).

[6]B. Smaller, Phys. Rev. 83, 812 (1951).

[7]R. V. Pound, Rev. Sci. Instrum. 17, 490 (1946).

[8]R. G. Brewer, Phys. Today 30, No. 5, 50 (1977).

[9]R. G. Brewer, in *Frontiers in Laser Spectroscopy,* edited by R. Balian, S. Haroche, and S. Liberman (North-Holland, Amsterdam, 1977), Vol. 1, p. 341.

[10]A. Schenzle and R. G. Brewer, Phys. Rev. A 14, 1756 (1976).

[11]A. Schenzle and R. G. Brewer, Phys. Rep. (Sec. C of Phys. Lett.) 43, No. 12, 455 (1978).

[12]J. Reid and T. Oka, Phys. Rev. Lett. 38, 67 (1977).

[13]S. Haroche and F. Hartmann, Phys. Rev. A 6, 1280 (1972).

[14](a) V. S. Letokhov and V. P. Chebotayev, *Nonlinear Laser Spectroscopy* (Springer, New York, 1977), p. 78; (b) R. G. DeVoe and R. G. Brewer (unpublished).

[15]T. Muramoto, S. Nakaniski, and T. Hashi, Opt. Commun. 21, 139 (1977); R. M. Macfarlane and R. M. Shelby, Opt. Lett. 6, 96 (1981), and references therein.

[16]W. Lenth, C. Oritz, and G. C. Bjorklund, Opt. Lett. 6, 351 (1981).

[17]M. Born and E. Wolf, *Principles of Optics,* 5th ed. (Pergamon, Oxford, 1975).